Chapter 3

Observation of the Weak Antilocalization and Linear Magnetoresistance in Topological Insulator Thin Film Hall Bar Device

Sunil Kumar Pradhan and Ranjan Barik

Additional information is available at the end of the chapter

http://dx.doi.org/10.5772/intechopen.76900

Abstract

In this research work, without using any resist and lithography techniques, we report clean, surface protected and high quality Topological Insulator (TI) thin film Hall Bar device of millimeter size long. In the magnetotransport measurements, the pronounced effect of weak antilocalization (WAL) behavior has been observed at low temperatures over the range T = 4–10 K and in the low field regions and the WAL cusp disappears as we go from 10 K onwards to higher temperatures, also we find that the high-field magenetoresistance (MR) is linear in field. With respect to magnetic field (B), the MR behavior seems to be symmetric. We also analyze the thickness dependent weak antilocalization (WAL) behavior, which has been observed in Topological Insulator Bi_2Te_3 thin film Hall Bar device. For varying thickness, our systematic magnetotransport measurements reveal WAL signals obtain in thicker films whereas below the critical thickness of ~4 nm, a sudden diminishment of the surface transport has been observed by suppression of WAL behavior. The analyzed and pronounced behavior of this effect is also greatly dependent on the temperatures, where the WAL cusps are observed in the low-field regions and at low temperatures.

Keywords: topological insulator, Bi_2Te_3, weak antilocalization, linear magnetoresistance

1. Introduction

In the recent years because of unique feature of topologically protected surface states which have strong spin-orbit coupling the three-dimensional (3D) topological insulators (TIs) like Bi_2Se_3, Bi_2Te_3 and their counterpart alloys have attracted tremendous and intense research

IntechOpen

© 2018 The Author(s). Licensee IntechOpen. This chapter is distributed under the terms of the Creative Commons Attribution License (http://creativecommons.org/licenses/by/3.0), which permits unrestricted use, distribution, and reproduction in any medium, provided the original work is properly cited.

attention [1–4]. The surface states which has been observed, are believed to be protected against time-reversal-symmetry, owing to the fact that, electrons in the surface state behave as dirac electrons as in case of 3D TI [5], which can be applied to spintronics devices [6], quantum computing [7] and it is necessary to investigate TI from the transport point of view in order to address the electronic properties of Dirac electrons. In terms of weak antilocalization (WAL) effect in thin films [8, 9], nanoribbons [10] and 3D TI crystals [11, 12], several research groups have already analyzed this transport behavior, by making small scale devices using conventional lithography techniques, but no paper has yet reported to observe this magneto-transport behavior in Bi_2Te_3 thin film Hall Bar device without using lithography techniques. Also in terms of potential applications in magnetic sensors and magnetic random access memory [13], materials exhibiting linear magnetoresistance (LMR) are found to be promising candidates. The linear MR behavior in Bi_2Se_3 [14, 15] and Bi_2Te_3 [16, 17] has been revealed in recent literatures and these TIs provide an ideal platform to study the origin of LMR because of the unique surface states that are naturally zero band gaps with linear dispersion.

It is necessary to grow a high quality TI thin film, in order to observe this magnetotransport behavior in topological insulator Bi_2Te_3. Molecular beam epitaxy (MBE) in this respect has demonstrated and found to be suitable in producing samples with carrier mobilities higher than the bulk crystals with precise control on the growth rate, out of modern thin film growth techniques. In order to realize layer by layer growth and obtaining the right stoichiometry [18] this technology is very important. Here, with respect to weak antilocalization (WAL) and magnetoresistance (MR), we report on the magnetotransport measurement. After fabrication, the thin film Hall Bar device is subjected to Physical Property Measurement System (PPMS), where the magnetic field is applied perpendicular to the plane of Hall Bar device. At programmed temperatures, by sweeping the magnetic field between −9 T and + 9 T, the Longitudinal Resistance is measured.

2. Experimental

Using Molecular Beam Epitaxy (MBE), the thin films of Bi_2Te_3 were grown on 7 × 7 mm dimension Al_2O_3 (0001) substrate. Prior to the deposition, the base pressure was maintained at ~ 8 × 10^{-10} mbar. To evaporate Bi (99%) and Te (99.9%) sources, the standard Knudsen diffusion cells were used and the Te and Bi were heated to 205 and 630°C respectively. At last at Te/Bi flux ratio of ~10 with a growth rate of 8 Å per minute the Bi_2Te_3 Thin films were prepared at a substrate temperature of 230°C. By defining the pattern, using standard lithographic techniques like electron-beam lithography or photolithography, numerous methods in the recent literatures [19–22] were reported in making thin film hall bar geometry but in our work, without using any resists and lithography techniques, we applied a clean method of making a topological insulator thin film hall bar device. In our device fabrication, we employed two physical masks, for the same sample holder. One for using in reactive ion etching (RIE), called etching mask and other for depositing metal electrodes, called metal mask. For defining the dimension of the thin film hall Bar, the etching mask served the purpose and the metal mask served the purpose of depositing the metal electrodes. After the

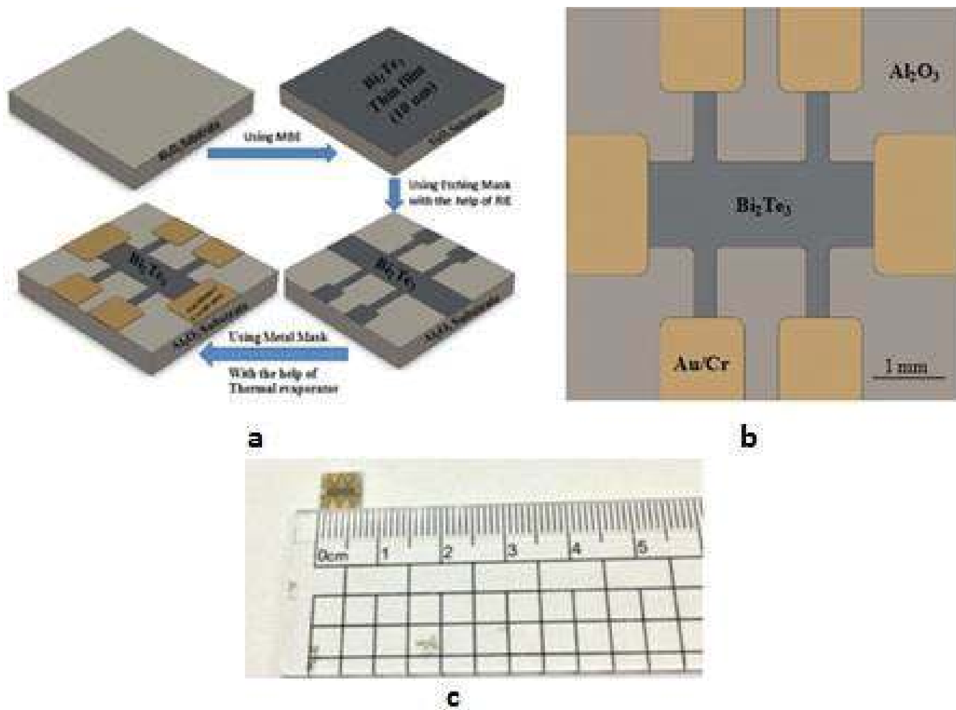

Figure 1. Methodology of fabrication of topological insulator Bi_2Te_3 thin film hall bar device.

thin film sample synthesized from the MBE, with the help of RIE the thin film hall Bar was made, using the etching mask placed over the sample on the sample holder. With the aid of CF_4 gas for 30 s, the etching was done for getting the required Hall Bar structure. Finally, on the same sample holder, Au (40 nm)/Cr (40 nm) metal ohmic contacts were made with the help of thermal evaporation, using the metal mask over the thin film Hall Bar sample. With dimension of 2 mm long and 1.5 mm wide we obtained our fabricated Topological Insulator Bi_2Te_3 thin film Hall Bar device. The **Figure 1a** shows the Schematic diagram of the device fabrication with image of Bi_2Te_3 topological insulator thin film hall bar device and the 7 × 7 mm dimension of the thin film hall bar device in **Figure 1b** and **c**, respectively.

3. Characterizations

Using AFM in a tapping mode, the topography of thin films was evaluated and by scanning a scratch deliberately made on as-grown thin films, the thickness was reliably determined. With the help of Siemens D-500 X-ray Diffractometer (XRD) further structural analyses were also carried out. In **Figure 2b** and **c** representative topographic AFM images of Bi2Te3 thin films are shown respectively, suggesting a layer-by-layer growth mode, revealing the ultra-smooth

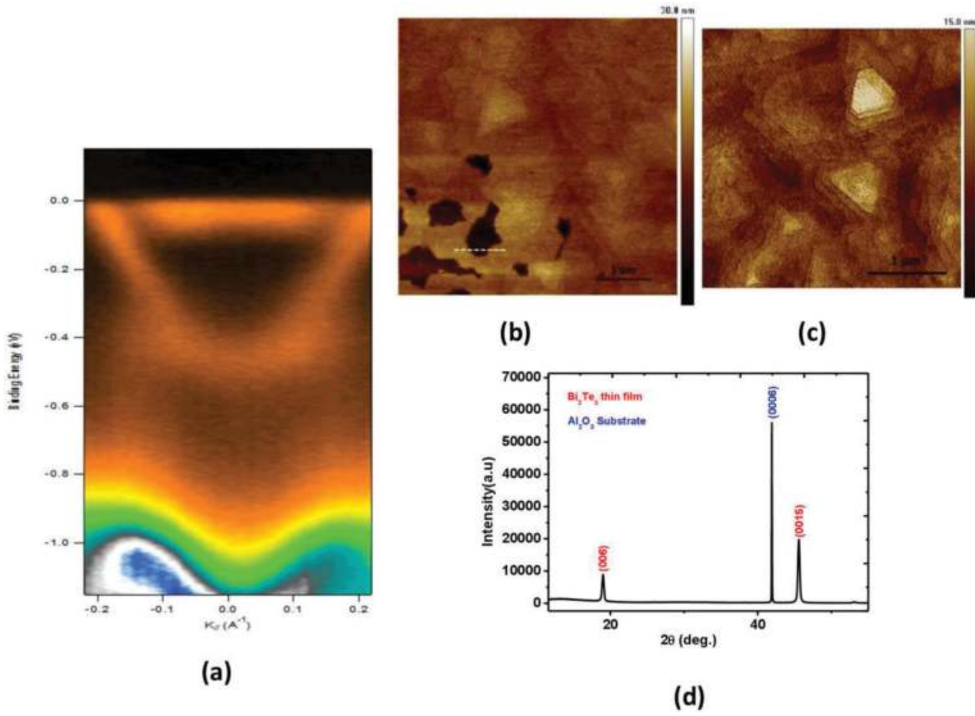

Figure 2. Characterization evidences of topological insulator Bi_2Te_3 thin film.

surfaces with large area terraces. In **Figure 2b**, the dashed line drawn, reveals 10 nm thickness film and **Figure 2c** illustrates 10 nm thin film, by the formation of 4–5 stacked layer comprising of domains of triangular terraces. This suggests a favorable growth dynamics accounting for the high crystalline quality of Topological Insulator thin film on Al_2O_3 substrate with the absence of spirals on the terraces together with the shape of the terrace. The XRD experiments were further conducted to investigate the crystalline quality and orientations. With the diffraction peak from Al_2O_3 substrate, **Figure 2d** displays (003) family diffraction peak from Bi_2Te_3 thin film. The result of the Angle Resolved Photo Emission Spectroscopy (ARPES), implying strong surface states is shown in **Figure 2a**.

4. Results and discussion

4.1. Magnetotransport measurement

In our observation and study, we confirm the weak antilocalization (WAL) effect and the origin of this research phenomenon is investigated. If we consider, interaction between time-reversal pair of electronic waves, then there is a constructive interference of this two phase-coherent

http://dx.doi.org/10.5772/intechopen.76900

electronic waves propagating in opposite directions along the same closed path, in the absence of spin-orbit interaction, which gives rise to Weak-Localization (WL) effect. This effect gives results in increase of resistance or decrease of conductance. But the constructive interference is broken as a result of a phase difference between the two electronic waves, when the magnetic field is applied perpendicular to the plane of the system. By increasing the magnetic field, the increase of resistance can gradually be removed and consequently negative magnetoresistivity occurs. It finally gives rise to increase of the resistance or reduction in the conductance around zero magnetic field as the resistance correction influenced by this localization. In the presence of the spin-orbit interaction, there is a significant enhancement in the resistance, which is known as weak antilocalization effect [23, 24]. As far as the quality of the grown thin film is concerned, it has significant impact on the studies of transport properties of charge carriers and the weak antilocalization (WAL) behavior is an evaluation and indication for such improvement in the quality of the thin film, which manifests both the Dirac nature of the surface states in the bulk of Topological Insulators [8, 25] and strong spin-orbit interaction. If we Compare the 2D electron system, the 2D surface state of the three-dimensional topological insulator is different [26] as an odd number of Dirac points are considered to be encircled by Fermi arc [27, 28]. If we evaluate the topological insulator, its surface remains metallic and cannot be localized by disorder [29]. By Hikami et al. [30], the surface state of the topological insulator is well described. The **Figure 3a** shows the results of the magnetotransport measurement for the temperature ranges from T = 4 to 100 K and fields up to 9 T. The pronounced effect of WAL cusps are marked at low temperature between 4 and 10 K and in the low field regions as shown in the **Figure 3a**. Also we observe the enhancement of peak and the dip structure behaviors in the magnetoresistance, which is quite remarkable with decreasing temperatures. We have defined the normalized magnetoresistance (MR) as a function of magnetic field as MR = [[R (B) − R (0)]/R (0)] × 100%., where R (B) and R (0) are the resistances at field B and at zero field, respectively. The WAL cusps disappear, as the temperature is increased from 10 K onwards. We observe the WAL characteristic behaviors in the temperature ranges from 4 to 10 K as shown in the **Figure 3a**, and disappearance of WAL cusp from 10 K onwards. The MR curves seems to be quadratic like B dependence at low fields between 2 and 6 T and at higher fields from 6 T onwards, the MR follows linear like behavior and does not saturate. The quadratic growth here can be well explained and analyzed by semi-classical model, where the magnetic field drifts the conduction electrons and these conduction electrons are deflected by the Lorentz force. At T = 4 K, the thickness dependent WAL behavior is shown in the **Figure 3b** showing the WAL cusps for 10, 20, 50 nm thickness film, where as there is no observable WAL effect in ultra-thin films like 4 and 2 nm and the magnetoresistance (MR) curve attains to be flat w.r.t. magnetic field (B). The Fermi level is not in the gap but crosses the Surface State, as the film is thinned enough. Hence, the observed drastic suppression of the surface transport is likely due to an enhanced scattering of the carriers. The phase breaking length (L_φ), which is of temperature dependence is extracted from the Hikami-Larkin-Nagaoka (HLN) model fit [30] for 10 nm thickness film is shown in the **Figure 3c**, which reveals the relatively large phase coherent length of 155.8 nm at 4 K, by fitting to the HLN model. The **Figure 3d** shows the Conductance change with respect to low magnetic field region with the HLN model fit for 10 nm thickness film.

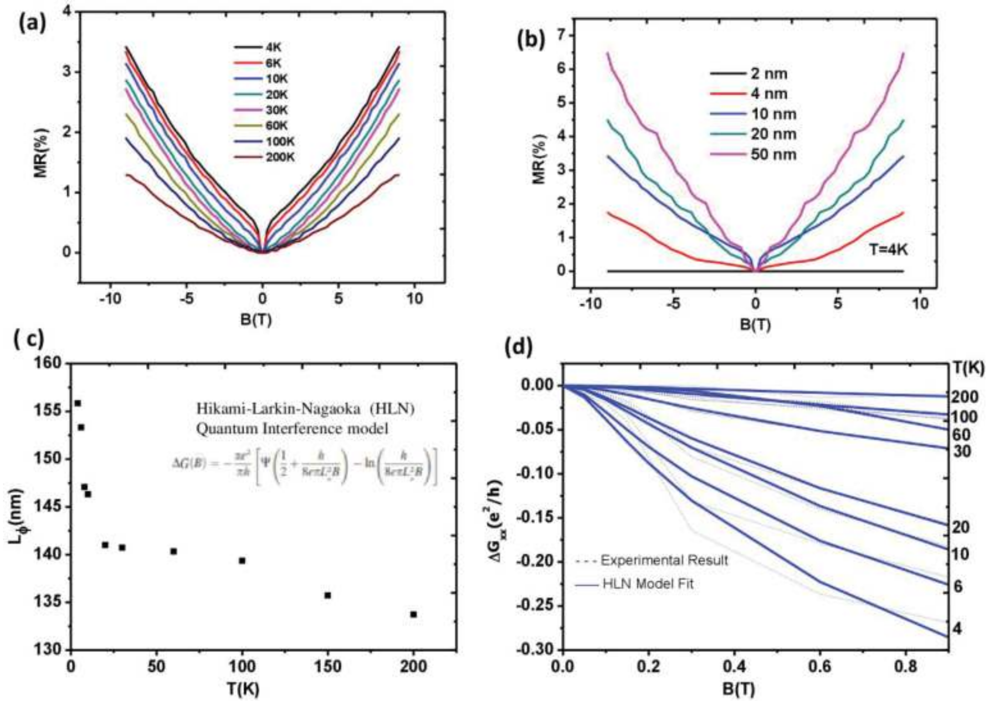

Figure 3. Results of Bi_2Te_3 thin films hall bar device with respect to magnetotransport.

4.2. Linear magnetoresistance (LMR)

We have observed linear magnetoresistance (LMR) behavior as shown in the **Figure 4** in our magnetotransport measurement study and it is found that the observed behavior is found to be seen in higher fields in the ranges from 6 to 9 T. In this linear region, there is a little variation in the slope of $d\text{MR}/dB$ with respect to temperatures. We have observed these linear and non-saturating magnetoresistance features in the temperature ranges from 2 to 20 K. Previous literatures show the same trends and results where the high field LMR was found in single crystal of YPdBi Heusler topological insulator [31] and in Bi_2Se_3 nanoribbons [15]. The topological surface states are manifested by these results. The Linear MR at strong magnetic field is expected to occur in the quantum limit in the linear energy spectrum, in which all the electrons populated into single Landau level as per the theory, proposed by Abrikosov [32, 33]. This is governed and satisfied by the inequality relation $(h/2\pi) \times W_c > E_f$, where $(h/2\pi) \times W_c$ is the cyclotron energy and E_f is the Fermi energy. So the weak temperature dependence is predicted by quantum LMR theory. However, recent literature shows that linear magnetoresistance (LMR) appears to occur in smaller magnetic field, where several Landau levels are populated by electrons [34]. There are some other research literatures, where it is analyzed that LMR at the high field as a consequence of closing of band gap under certain pressure. This profound alteration of band structure is

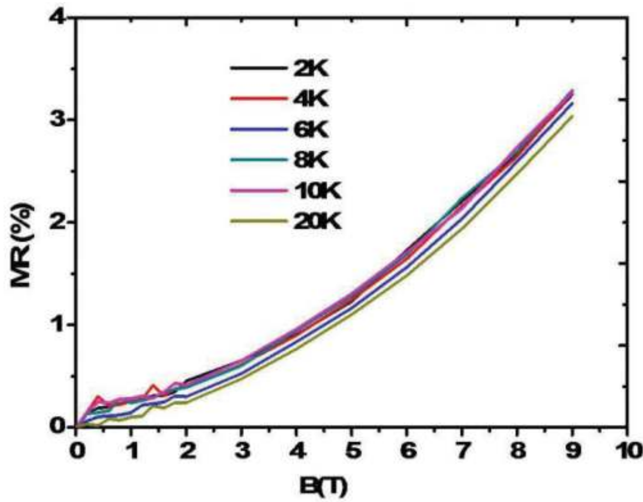

Figure 4. LMR of Bi_2Te_3 thin film hall bar device at high fields.

found in silver rich or silver deficient chalcogenides [35] by the application of hydrostatic pressure. Hence, the gap less linear energy spectrum, which is suggested by this, such as the surface states of topological insulators is required for the observation of Linear MR in high fields. As there exists a bulk band gap for the bulk state, in this analysis, the possible bulk contribution in the quantum LMR is excluded. To the previous literature on topological insulator B_2Te_3 nano-sheets [17], our results in linear MR are quite similar. As shown in the **Figure 4**, in our study we report ≅ 3.2% MR value for temperatures ranging from 2 to 20 K. This characteristic feature of Linear MR (LMR), which has been found to be proportional to the magnetic field (B), is suitable for application in high magnetic field sensors.

4.3. Temperature-dependent electrical resistance measurement

For observing the temperature dependent resistance, we did the electrical measurements in our study. The longitudinal resistance (R) at zero magnetic field as a function of temperature is shown in the **Figure 5**. From the figure it is evident that, there is a decrease in the resistance in the temperature range from 300 to 240 K. The reason, we can consider with the bulk band gap. With the recent report on the ARPES measurements analysis of Bi_2Se_3 thin film grown on SiC (0001) by MBE [36], where there is a progressive and systematic increase in the bulk band gap with reducing film thickness, it implies the quantum confinement of the film along the growth direction perpendicular to the substrate. As in our case, the grown film is thin enough, so the result is quite practical and evident at higher temperatures. The longitudinal resistance decreases as the temperature decreases from 240 to 4 K, resembling the metallic like behavior as observed in most of the topological Insulators [37]. Such trend of decrease with temperatures can be analyzed and explained by power law increase of mobility with temperatures and alleviated phonon scattering. The resistance attains to be constant value

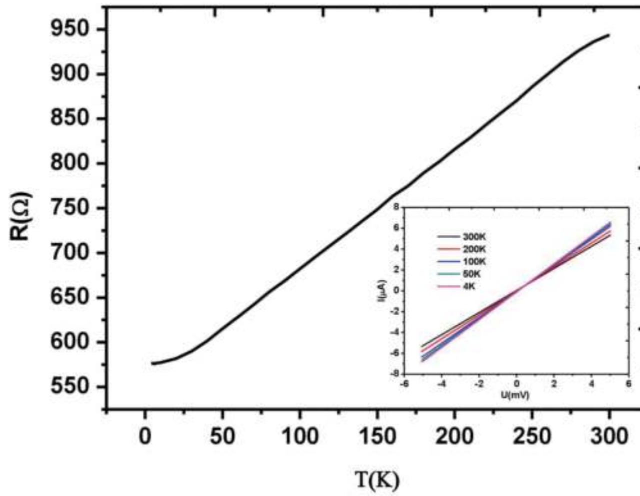

Figure 5. Temperature-dependent electrical resistance measurement result of Bi_2Te_3 hall bar device.

in the temperature range between 4 and 2 K. The reason, where the transport is primarily governed by combination of surface states and impurity band conduction is considered to be bulk carrier's freeze out effect. To the previous literature on Bi_2Se_3 grown on Si substrate [38], this temperature dependent result is quite similar. The Current-Voltage curves at different temperature, indicating ohmic contacts over the whole range of temperatures is shown in the insert in the **Figure 5**.

5. Conclusion

In the summary, in our fabricated topological insulator Bi_2Te_3 thin film Hall Bar device, we report the observation of weak antilocalization (WAL) behavior and linear magnetoresistance (LMR). The WAL characteristics is found to be in the low temperature and in the low magnetic field region and the LMR is considered to be accompanied with gapless energy spectrum of surface Dirac fermions and is believed to be quantum origin. A dip near 0 T magnetic fields is observed in the magnetoresistance (MR) characteristics of Bi_2Te_3 thin film hall Bar device. The originated dip is from the WAL effect and is found to be at low temperatures. By fitting to the HLN model for 10 nm thin film, we also derive relatively large phase breaking length of 155.8 nm at 4 K. This dependence on the thickness of the thin film has a pronounced behavior, i.e., below a certain critical thickness there is no observable WAL behavior. In our study and analysis, we observe disappearance of WAL in <5 nm thickness film. The reason is the film of topological insulator is so thinned that it leads to an opening of the gap at the Dirac point and results in a degenerate, massive Dirac dispersion, which leads to the diminishment of surface transport, by the observing flatness in the magnetoresistance curve.

http://dx.doi.org/10.5772/intechopen.76900

Acknowledgements

The help and resources received from Department of Engineering and System Science, National Tsing Hua University, Taiwan and Central Electronics Engineering Research Institute, Pilani are thankfully acknowledged.

Author details

Sunil Kumar Pradhan[1]* and Ranjan Barik[2]

*Address all correspondence to: sunilpradha@gmail.com

1 Department of Engineering and System Science, National Tsing Hua University, Hsinchu, Taiwan (ROC)

2 Microwave Tube Division, CSIR-Central Electronics Engineering Research Institute, Pilani, Rajasthan, India

References

[1] Langbehn J, Peng Y, Trifunovic L, von Oppen F, Brouwer PW. Physical Review Letters. 2017;**119**:246401

[2] Song Z, Fang Z, Fang C. Physical Review Letters. 2017;**119**:246402

[3] Benalcazar WA, Bernevig BA, Hughes TL. Science. 2017;**61**:357

[4] Chiu C-K, Teo JCY, Schnyder AP, Ryu S. Reviews of Modern Physics. 2016;**88**:035005

[5] Xu Y, Chiu J, Miao L, He H, Alpichshev Z, Kapitulnik A, Biswas RR, Wray LA. Nature Communications. 2017;**8**:14081

[6] Lee I, Kim CK, Lee J, Billinge SJ, Zhong R, Schneeloch JA, Liu T, Valla T, Tranquada JM, Gu G, Davis aJ CS. Proceedings of the National Academy of Sciences of the United States of America. 2015;**112**:1316

[7] Lau A, van den Brink J, Ortix C. Physical Review B. 2016;**94**:165164

[8] Chen J, He XY, Wu KH, Ji ZQ, Lu L, Shi JR, Smet JH, Li YQ. Physical Review B. 2011;**83**:241304

[9] Onose Y, Yoshimi R, Tsukazaki A, Yuan H, Hidaka T, Iwasa Y, Kawasaki M, Tokura Y. Applied Physics Express. 2011;**4**:083001

[10] Qu F, Yang F, Chen J, Shen J, Ding Y, Lu J, Song Y, Yang H, Liu G, Fan J, Li Y, Ji Z, Yang C, Lu L. Physical Review Letters. 2011;**107**:016802

[11] Murani A, Kasumov A, Sengupta S, Kasumov YA, Volkov VT, Khodos II, Brisset F, Delagrange R, Chepelianskii A, Deblock R, Bouchiat H, Gu’eron S. Nature Communications. 2017;**8**:15941

[12] Black-Schaffer AM, Balatsky AV, Fransson J. Physical Review B. 2015;**91**:201411

[13] Deb O, Soori A, Sen D. Journal of Physics. Condensed Matter. 2014;**26**:315009

[14] He H et al. Applied Physics Letters. 2012;**100**:032105

[15] Tang H, Liang D, Qiu RLJ, Gao XPA. ACS Nano. 2011;**5**:7510

[16] Li W, Claassen M, Chang C-Z, Moritz B, Jia T, Zhang C, Rebec S, Lee J, Hashimoto M, Lu D-H, Moore RG, Moodera JS, Devereaux TP, Shen Z-X. Scientific Reports. 2016;**6**:32732

[17] Wang XL, Du Y, Du SX, Zhang C. Physical Review Letters. 2012;**108**:266806

[18] Zhang GH, Qin HJ, Teng J, Guo JD, Guo Q, Dai X, Fang Z, Wu KH. Applied Physics Letters. 2009;**95**:053114

[19] He H et al. Applied Physics Letters. 2012;**100**:032105

[20] Kim D, Syers P, Butch NP. Nature Communications. DOI: 10.1038/ncomms3040. https://www.nature.com/articles/ncomms3040.pdf

[21] Yan Y et al. Applied Physics Letters. 2013;**103**:033106

[22] Zhang G, Qin H. Advanced Functional Materials. 2011;**21**:2351

[23] Chang C-Z, Tang P, Wang Y-L, Feng X, Li K, Zhang Z, Wang Y, Wang L-L, Chen X, Liu C, Duan D, He K, Ma X-C, Xue Q-K. Physical Review Letters. 2014;**112**:056801

[24] Chang C-Z, Zhao W, Kim DY, Zhang H, Assaf BA, Heiman D, Zhang S-C, Liu C, Chan MH, Moodera JS. Nature Materials. 2015;**14**:473

[25] Steinberg H, Laloe JB, Fatemi V, Moodera JS, Jarillo-Herrero P. Physical Review B. 2011;**84**:233101

[26] Ma Y, Kou L, Dai Y, Heine T. Physical Review B: Condensed Matter and Materials Physics. 2016;**94**:201104

[27] Qi XL, Zhang SC. Reviews of Modern Physics. 2011;**83**:1057

[28] Bian G, Wang Z, Wang XX, Xu C, Xu S, Miller T, Hasan MZ, Liu F, Chiang TC. ACS Nano. 2016;**10**:3859-3864

[29] Ando Y, Fu L. Annual Review of Condensed Matter Physics. 2015;**6**:361-381

[30] Hikami S, Larkin AI, Nagaoka Y. Progress in Theoretical Physics. 1980;**63**:707

[31] Wang W, Du Y. Scientific Reports. 2013;**3**:2181

[32] Niu C, Buhl PM, Bihlmayer G, Wortmann D, Blügel S, Mokrousov Y. Nano Letters. 2015;**15**:6071-6075

[33] Zhang RW, Zhang CW, Ji W-X, Li P, Yan S-S, Wang P-J. Scientific Reports. 2016;**6**:21351

[34] Zhang R-W, Zhang C-W, Ji W-X, Li P, Wang P-J, Yan S-S. Applied Physics Letters. 2016;**109**:182109

[35] Luo W, Xiang H. Nano Letters. 2015;**15**:3230-3235

[36] Zhou L, Shi W, Sun Y, Shao B, Felser C, Yan B, Frauenheim T. 2D Mater. 2016;**3**:035018

[37] Si C, Jin K-H, Zhou J, Sun Z, Liu F. Nano Letters. 2016;**16**:6584-6591

[38] Zhao J, Li Y, Ma J. Nanoscale. 2016;**8**:9657-9666